Available online at www.sciencedirect.com
ScienceDirect
Ceramics International 35 (2009) 1999–2005
CERAMICS INTERNATIONAL
www.elsevier.com/locate/ceramint

Investigation of substrate bias effects on the reactively sputtered ZrN diffusion barrier films

Jian-Long Ruan [a], Ding-Fwu Lii [b], J.S. Chen [a], Jow-Lay Huang [a,c,*]

[a] Department of Materials Science and Engineering, National Cheng-Kung University, Tainan 701, Taiwan, ROC
[b] Department of Electrical Engineering, Cheng Shiu University, Kaohsiung 833, Taiwan, ROC
[c] Department of Polymer Materials, Kun Shan University, Yung-Kang City, Tainan Hsien 710, Taiwan, ROC

Received 5 September 2008; received in revised form 29 September 2008; accepted 7 November 2008
Available online 3 December 2008

Abstract

ZrN diffusion barrier films were prepared by DC reactive magnetron sputtering under different negative substrate bias. The composition, microstructure, resistivity and diffusion barrier properties of ZrN films, with respect to substrate bias, were studied by means of X-ray diffraction, electron probe microanalyzer, Auger electron spectroscopy, and four point probe method. Results showed that the deposition rate and impurity oxygen content of ZrN films were substantially influenced by the resputtering effects due to the ion bombardment on the film surface. The competition between surface energy and strain energy made the preferred orientation of ZrN films change from (1 1 1) to (2 0 0) and then back to highly (1 1 1) preferred orientation as a function of substrate bias. The application of negative substrate bias could effectively decrease the electrical resistivity due to the decrease of impurity oxygen content and the densification of films, resulting from the moderate-energy ion irradiation. The biased ZrN films could successfully be used as a diffusion barrier layer, between Cu and SiO_2, even up to the high temperature of 800 °C for 30 min.

Keywords: A. Films; C. Electrical properties; D. Nitrides; Diffusion barrier

1. Introduction

With increasing demands for faster and smaller electronic devices in ultra large scale integrated circuits (ULSI), copper with a low resistivity and a superior electromigration resistance is a promising conduct material compared with conventional aluminum (Al) [1]. However, with a higher diffusivity than Al, Cu diffused easily through the dielectrics, and then, the performance of devices was degraded by the introduction of deep-level acceptor [2]. Moreover, Cu silicides were easily formed at temperatures as low as 200 °C. Therefore, there is a need to develop an ultra thin effective diffusion barrier layer for preventing of copper diffusion. Owing to the challenge of reducing the total resistance of the fine Cu interconnects, while still maintaining high reliability, requirements for diffusion barriers which are applicable to Cu metallization, in decreased dimensions, become rigorous. Essentially, the demands for diffusion barrier in Cu interconnection technology include an extreme thermal stability and a low resistivity.

Binary transition metal nitrides, such as TiN and TaN, have been widely investigated as diffusion barriers for Cu metallization due to their relatively high melting point, high thermal stability, low resistivity, and good adhesion properties [3,4]. In conventional Al-based metallization, TiN is the most commonly used barrier materials. Unfortunately, TiN cannot provide enough Cu barrier performance, since Cu and Ti form a bulk alloy, and a Cu grain boundary diffusion proceeds readily in TiN [5,6]. For Cu metallization, Ta and TaN have been widely recognized as an attractive diffusion barrier, because Ta is thermally stable with respect to Cu. Cu and Ta are almost completely immiscible up to their melting point and do not react with each other [7]. In addition, the formation of amorphous structure in Ta–N system is also beneficial for improving the barrier performance due to the lack of grain

* Corresponding author at: Department of Materials Science and Engineering, National Cheng Kung University, No. 1, University Road, Tainan 701, Taiwan, ROC. Tel.: +886 6 2348188; fax: +886 6 2763586.
E-mail address: jlh888@mail.ncku.edu.tw (J.-L. Huang).

0272-8842/$34.00
doi:10.1016/j.ceramint.2008.11.002

boundary diffusion paths [8]. Although TaN films exhibit an excellent barrier property against Cu at high temperatures, it seems that TaN films are still unsatisfactory for using as diffusion barrier in the future 45 nm technology node, due to the high resistivity (about 2 μΩ m) of TaN films [9–10].

Among the transition metal nitrides, ZrN is a promising candidate for diffusion barriers due to its lowest electrical resistivity (0.136 μΩ m for bulk) and a negatively larger heat of formation (−365 kJ/mol), compared with those of TiN (−336 kJ/mol) and TaN (−251 kJ/mol) [11,12]. It is generally suggested that materials with negatively larger heat of formation may have better thermal stability. According to Takeyama et al. [11], the reactively sputtered ZrN films with thickness of 140 nm between Cu and Si are fairly stable upon annealing at 750 °C in a vacuum (1.33×10^{-5} Pa) for 1 h. In order to satisfy the increasing demands for thinner barrier thickness in the future semiconductor technology, some researchers have studied the barrier properties of ZrN films with much thinner thickness. It has been reported that the ZrN films, prepared by atomic layer deposition with 15 nm thickness, can be satisfactorily stable up to 550 °C in a vacuum (1.33×10^{-4} Pa) for 1 h [3]. Furthermore, Sato et al. [13] have examined the barrier performance of reactively sputtered ZrN films, with 5 nm thickness, between Cu and SiOC low-*k* insulating layer and reported that the extremely thin barrier can tolerate annealing at 500 °C, in a vacuum (1.33×10^{-5} Pa), for 30 min.

It seems that the barrier performance of extremely thin ZrN films can be improved further because the failure temperature reported in the previous studies is just above 500 °C [13,14]. In addition, the resistivity of ZrN is lower than that of TaN. Therefore, ZrN has been proposed to be used as a diffusion barrier layer between Cu and SiO_2 instead of TaN in this study. ZrN diffusion barrier films were prepared by reactive DC magnetron sputtering, and the effects of negative substrate bias on the microstructure, resistivity, and diffusion barrier performance of the ZrN films were intensively studied.

2. Experimental procedure

N-type silicon (1 0 0) wafers with a resistivity of 0.01–0.1 Ω m were degreased in organic baths and chemically etched, with dilute HF solution, to remove the native oxide. Subsequently, thermal SiO_2 with 100 nm thickness was grown by oxidizing Si wafers in dry oxygen at 1050 °C. ZrN thin films were deposited onto Si substrates with a 100 nm SiO_2 layer by DC reactive magnetron sputtering from a Zr target (99.7% in purity) of 76.2 mm diameter. A cryo-pump, coupled with a rotary pump, was used to achieve an ultimate pressure of 6.68×10^{-4} Pa, before introducing gas mixtures of Ar and N_2. The Zr target was pre-sputtered at 0.27 Pa in Ar for 10 min prior to film deposition for cleaning purpose. The working pressures were fixed at 0.27 Pa. The flow rates of Ar and N_2 were maintained at 40 and 3 sccm (which sccm denotes cubic centimeter per minute at STP), respectively, during the deposition process. The cathode DC power and target–substrate distance was kept at 150 W and 5 cm, respectively. A negative substrate bias voltage of 0–300 V was supplied to the substrate during deposition. The thickness of the ZrN films was kept at 100 nm for characterization analysis, while 10 nm for barrier performance evaluation, by properly adjusting the sputtering time. In addition, the copper layer (100 nm), over ZrN/SiO_2, was deposited at a DC power of 150 W and a total pressure of 0.27 Pa, under an Ar flow rate of 20 sccm, without bias voltage on the substrate. The prepared Cu (100 nm)/ZrN (10 nm)/SiO_2 (100 nm)/Si specimens were then annealed at temperatures between 700 and 900 °C for 30 min in a vacuum ($<4 \times 10^{-3}$ Pa).

The film thickness was measured by an α-step apparatus (Surface profiler, Tencor, USA). The deposition rate was calculated from the film thickness and deposition time. A field-emission electron probe micro-analyzer (FE-EPMA; JEOL JXA-8500F, Japan) was used to determine the chemical composition of deposited films. The phases, textures, lattice constant, and crystallite size of the films were analyzed by X-ray diffraction (XRD; Rigaku D/MAX2500, Japan) using Cu Kα radiation. The electrical resistivity of the films was measured by a four point probe (Model RT-7, Napson, Japan). A field emission gun scanning electron microscope (FEG-SEM, Philips XL-40FEG, Holland) was used to examine the surface morphology of the Cu/ZrN/SiO_2/Si samples after annealing. The depth profiles of the Cu/ZrN/SiO_2/Si samples before and after annealing were analyzed by Auger electron spectroscopy (AES; VG Microlab 310-D, UK).

3. Results and discussion

3.1. Deposition rate and composition

The deposition rate and oxygen content of ZrN films deposited under different substrate bias are plotted in Fig. 1. The results indicated that the deposition rate initially decreased abruptly and then gradually, with the increase of substrate bias. The decrease of deposition rate, with increasing substrate bias, was thought to be due to the removal of the impurities (oxygen and carbon), densification of films, and the resputtering of some deposited materials due to the energetic ion bombardment [14].

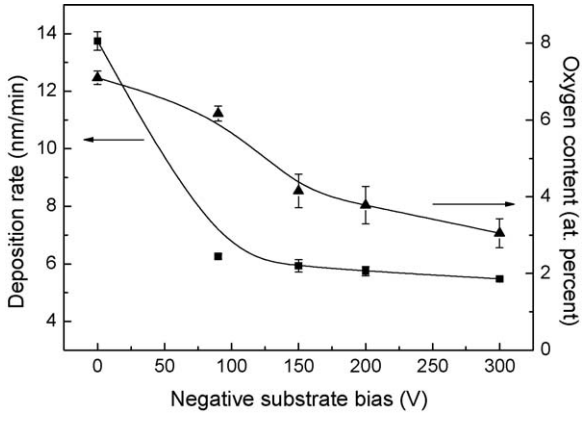

Fig. 1. Deposition rate and oxygen content of ZrN films with different substrate bias.

The quantitative composition analysis by FE-EPMA (not shown here) exhibited that the N/Zr atomic ratio was kept around the value about of 0.9 as a function of negative substrate bias. In addition, the existence of oxygen atoms in the ZrN films was also observed due to the presence of residual gas in the deposition chamber [15], originating from the low ultimate pressure (6.68×10^{-4} Pa) attained in the present work. The oxygen content in the films decreased with the increase of substrate bias (Fig. 1) due to the resputtering of the adsorbed impurity gas atoms by the energized ion bombardment [16]. Although the affinity of oxygen was higher than that of nitrogen to Zr, the amount of residual oxygen in chamber was too small to form a strong binding of zirconium oxide compound, during the deposition of ZrN films, while reactive nitrogen gas was sufficient to form the ZrN compound with zirconium, during film growth. Therefore, during the deposition of films, the residual oxygen may probably only adsorb on the growing film surface and it may be resputtered by the ion bombardment effects, causing the decrease of oxygen content with substrate bias. However, the similar resputtering phenomenon would not occur for nitrogen due to the formation of strong binding of ZrN compound.

3.2. Microstructure

X-ray diffraction (XRD) patterns of ZrN films with different substrate bias are shown in Fig. 2. All diffraction peaks pertained to crystal planes of ZrN phase (NaCl-type structure, ICDD PDF #35-0753). The XRD peaks of the films deposited with negative bias shifted to the lower values of 2θ angle. This indicated that the lattice constant of ZrN films with applied negative bias was larger than the ideal ZrN lattice constant (0.4578 nm) [17]. According to Bragg's law, the lattice constant of ZrN films, calculated from the θ angle, was about of 0.463 nm for all the bias values. The reason for the peak shift towards the lower 2θ angle was the residual compressive stress in films resulting from energetic ion bombardment [18].

In order to study the evolution of textures in ZrN films, the (1 1 1) texture coefficient was defined as the ratio of the (1 1 1) peak intensity to the sum of the (1 1 1) and (2 0 0) peak intensity in the XRD patterns. Same designation was for the (2 0 0) texture coefficient. The (1 1 1) and (2 0 0) texture coefficients calculated as a function of substrate bias are shown in Fig. 3 with two dashed lines representing the values for (1 1 1) plane (0.54) and (2 0 0) plane (0.46) from ZrN powders. Results showed that the preferred orientation of the ZrN films changed from (1 1 1) preferred to (2 0 0) preferred and then back to highly (1 1 1) preferred with the increase of substrate bias.

In NaCl-type structure, the (2 0 0) plane has the lowest surface energy while the (1 1 1) plane has the lowest strain energy [19]. The preferred orientation of such structure was determined by the lowest overall total energy conditions, resulting from a critical competition between surface energy and strain energy [20]. Similar to the report for RF sputtered TiN films [20], the (1 1 1) preferred orientation of the as-deposited ZrN films by DC sputter in this study was formed in order to reduce the overall energy by the generation of a relatively higher intrinsic stress and strain energy.

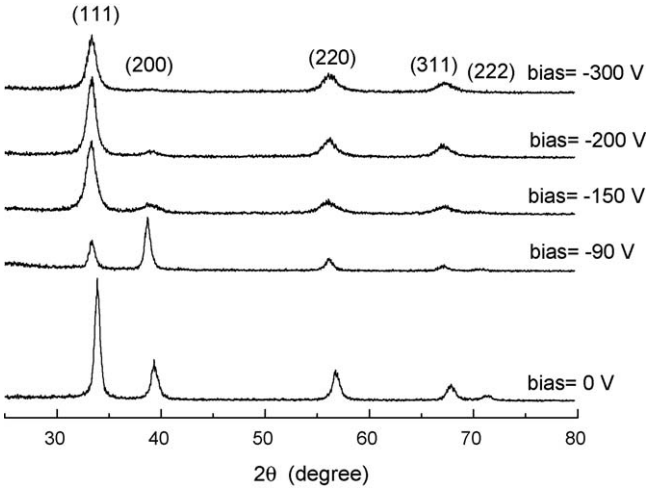

Fig. 2. X-ray diffraction patterns of ZrN films with different substrate bias.

Ensinger [21] reported that the growth of film under low-energy ion irradiation was substantially affected by the adatom mobility. In addition, Marinov [22] reported that the surface mobility of adatoms would be enhanced by the energized ion bombardment. Since the (2 0 0) plane has the lowest surface energy in NaCl-type structure [19], the adatoms with relatively higher surface mobility, caused by energized ion irradiation, could therefore stack with the lowest energy crystal facets parallel to the substrate, under low substrate bias condition. At higher bias voltage, the growing films could possibly suffer much heavier ion bombardment and consequently produced larger compressive stresses, leading to the much higher strain energy existing in the films [15,23]. Based on the anisotropy of elastic modulus for the crystal planes, it is expected that the strain energy is higher for the (2 0 0) than for the (1 1 1) plane [19]. Thus for the highly strained ZrN films deposited under higher bias voltage, the highly preferred (1 1 1) textures were formed in order to reduce the strain energy in the films.

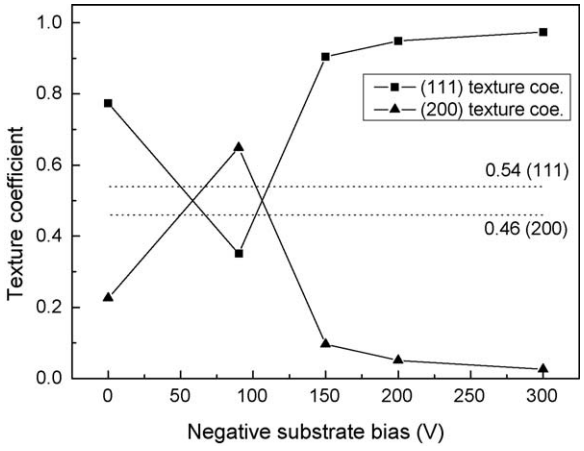

Fig. 3. (1 1 1) and (2 0 0) texture coefficient of ZrN films as a function of substrate bias.

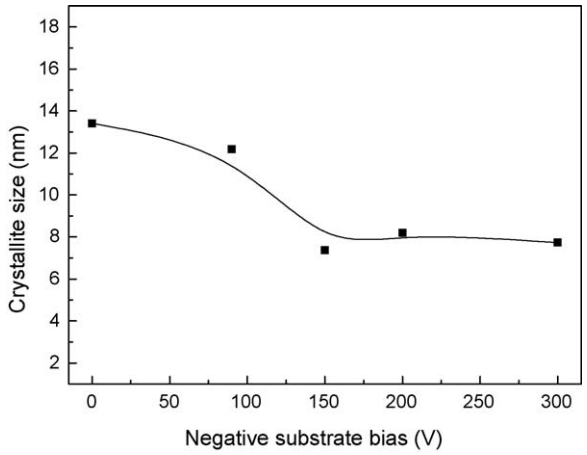

Fig. 4. Crystallite size of ZrN films with different substrate bias.

The crystallite size of ZrN films was calculated by the Scherrer's formula [24] from the integral width of (1 1 1) peaks in the XRD patterns. Fig. 4 shows the crystallite size of ZrN films with different substrate bias. With the increase of bias voltage, the crystallite size decreased due to the continuous renucleation of growing films, which was induced by the ion-irradiation generated defects [25]. Similar variation in the crystallite size with bias was also observed in the Cavaleiro's study [26].

3.3. Electrical resistivity

The electrical resistivity of ZrN films with different substrate bias is shown in Fig. 5. The resistivity continuously decreased to a minimum value of 1.3 μΩ m with the increase of substrate bias to −200 V and then increased again. The initial decrease of resistivity with negative substrate bias was due to the reduction of impurity oxygen content in the films (Fig. 1) and probably the densification of films resulting from ion bombardment [27]. Essentially, the decrease of impurity atoms content will reduce the electron scattering probability and then improve the electrical conductance of thin films [28]. In addition, the film densification is also beneficial for the electrical conductance of the films [29]. The increase of resistivity beyond the bias voltage of 200 V may be probably due to the increase of ion-induced defects, which were caused by the high-energy ion bombardment [30]. Although the resistivity was generally increased for the films with smaller grain size, the impurity oxygen content and the energy of ion bombardment should be the dominant factors in determining the resistivity of ZrN films deposited with negative substrate bias.

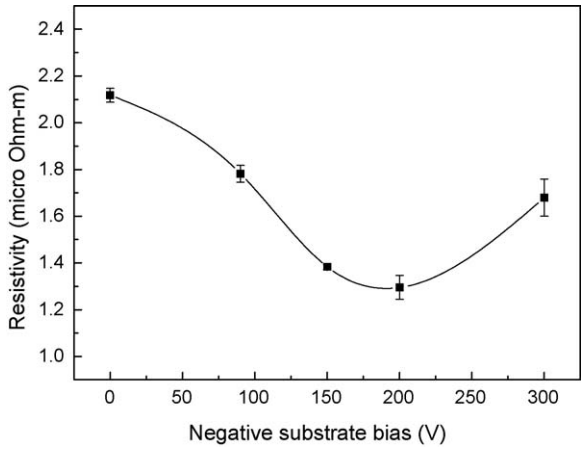

Fig. 5. Electrical resistivity of ZrN films with different substrate bias.

3.4. Barrier performance of Cu/ZrN/SiO_2/Si specimens

In order to investigate the feasibility of using ultra-thin ZrN films (10 nm) as diffusion barriers, both ZrN and Cu films were deposited onto Si substrates with a 100 nm SiO_2 layer to fabricate Cu (100 nm)/ZrN (10 nm)/SiO_2 (100 nm)/Si specimens. The heat treatments of the Cu/ZrN/SiO_2/Si specimens were carried out at temperatures between 700 and 900 °C for 30 min in a vacuum ($<4 \times 10^{-3}$ Pa). In order to satisfy the requirements of electrical conductance for diffusion barrier layer in Cu metallization, the specimens, with negative bias voltage of 200 V, were picked for the evaluation of barrier property comparing with that of the specimens without bias.

The XRD patterns of Cu/ZrN(0 V)/SiO_2/Si and Cu/ZrN(−200 V)/SiO_2/Si specimens, annealed at different temperatures (e.g. 0, 700, 800, 900 °C) for 30 min indicated that no peaks related to the compounds formed by a reaction between Cu and ZrN or underlayer SiO_2/Si could be observed. Only strong peaks related to the Cu films itself were shown for the specimens annealed up to 900 °C. As it was reported previously, the failure temperature was not precisely revealed by the XRD analysis because the new products (such as Cu silicides) formed by Cu diffusion might remain amorphous [4] or even be absent in the films.

Conversely, the four point probe measurements were sensitive to the impurity diffusion of Cu or other layer constituents, resulting in the precise indication of failure temperature. The sheet resistance of Cu/ZrN/SiO_2/Si specimens as a function of annealing temperature is shown in Fig. 6. The initial slight decrease of sheet resistance for both the Cu/ZrN(0 V)/SiO_2/Si and Cu/ZrN(−200 V)/SiO_2/Si structures

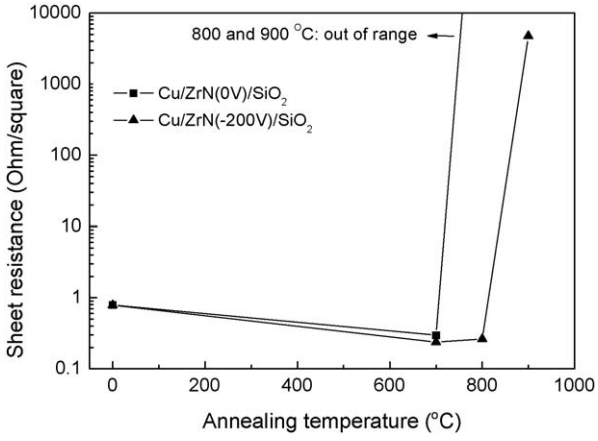

Fig. 6. Sheet resistance of Cu/ZrN/SiO_2/Si specimens as a function of annealing temperature.

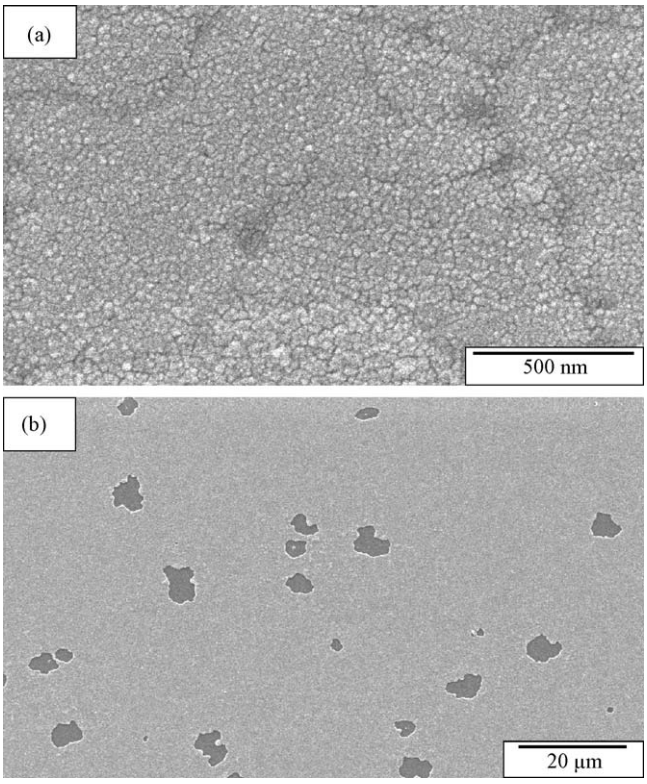

Fig. 7. SEM images of the top surface of Cu/ZrN(−200 V)/SiO_2/Si specimens after annealing at (a) 700 °C and (b) 800 °C.

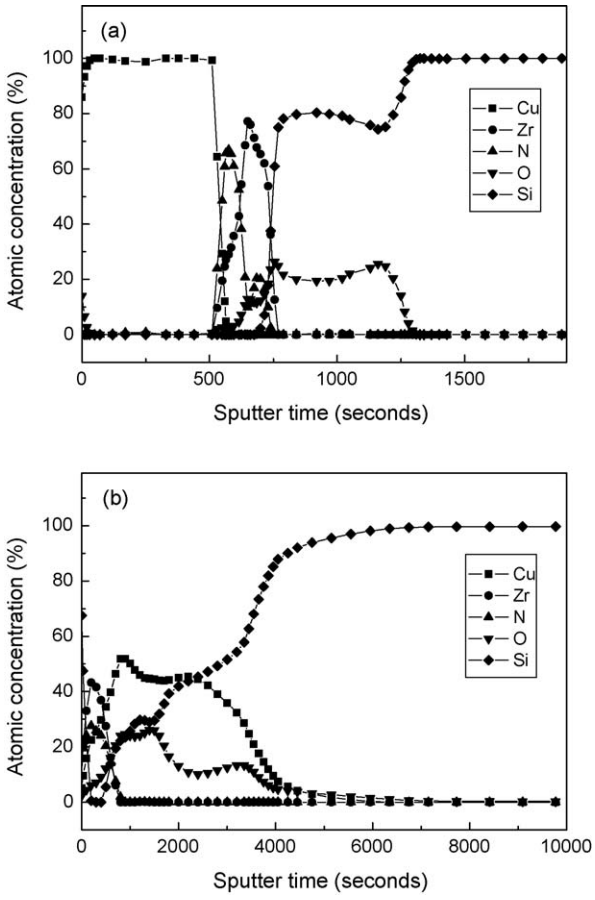

Fig. 8. AES depth profiles of Cu/ZrN(0 V)/SiO_2/Si structures: (a) as-deposited and (b) annealed at 800 °C for 30 min.

was most likely due to the grain growth and defect annihilations of Cu films during annealing [31]. Similar reduction in sheet resistance was also observed for Cu/TiN/Si structures [32]. A drastic increase in sheet resistance for the Cu/ZrN(0 V)/SiO_2/Si structure after annealing at 800 and 900 °C could be related to the interdiffusion and/or reaction of layer constituents [32]. However, the similar drastic increase in the sheet resistance could only be observed at 900 °C for the Cu/ZrN(−200 V)/SiO_2/Si structure. In addition, the sheet resistance of Cu/ZrN(−200 V)/SiO_2/Si structure only slightly increased after annealing at 800 °C. Fig. 7 shows the SEM images of the top surface of Cu/ZrN(−200 V)/SiO_2/Si specimens after annealing at (a) 700 and (b) 800 °C. The surface of Cu/ZrN(−200 V)/SiO_2/Si specimens after annealing at 700 °C simply showed the morphology of Cu grains. After annealing at 800 °C, broken holes appeared on the copper surface due to the Cu film agglomeration [33,34]. The formation of broken holes, on the copper film's surface, was thought to be responsible for the slight increase of sheet resistance after annealing at 800 °C.

AES depth profiles of the Cu/ZrN(0 V)/SiO_2/Si and Cu/ZrN(−200 V)/SiO_2/Si structures before and after annealing are shown in Figs. 8 and 9, respectively. Without calibration, the atomic concentrations presented here are only semi-quantitative. The as-deposited Cu/ZrN(0 V)/SiO_2/Si and Cu/ZrN(−200 V)/SiO_2/Si samples exhibited a well-separated stacked structure with distinct Cu/ZrN and ZrN/SiO_2 interfaces, as shown in Figs. 8(a) and 9(a). However, for the 800 °C annealed Cu/ZrN(0 V)/SiO_2/Si structures, the Cu signal extended into the SiO_2 layer; meanwhile, the outdiffusion of the Zr and N signal toward the sample surface occurred (Fig. 8(b)). The interdiffusion of Cu and the underlayer constituents made it difficult to distinguish the interfaces and then destroyed the well-separated stacked structure. By contrast, in the AES depth profiles of Cu/ZrN(−200 V)/SiO_2/Si samples annealed at 800 °C (Fig. 9(b)), the interfaces were fairly stable and the layered structure still preserved, although somewhat diffused distributions of elements were noticed as compared with the as-deposited samples (Fig. 9(a)). According to the comparison of AES analysis results (Figs. 8 and 9), it indicated that the barrier property of the ZrN(−200 V) films is better than that of ZrN(0 V) films. This is consistent with the sheet resistance results from Fig. 6.

In summary, the Cu/ZrN(0 V)/SiO_2/Si structure failed at annealing temperature of 800 °C for 30 min due to the interdiffusion between layers, while the Cu/ZrN(−200 V)/SiO_2/Si structure still survived. According to Park et al. [35], the diffusion barrier performance of TiN films could be improved in consequence of the film densification, resulting from ion bombardment during film growth. Therefore, the biased ZrN films with ultra thin thickness of 10 nm could be well used as a potential diffusion barrier for the future semiconductor technology, due to the moderate-energy ion

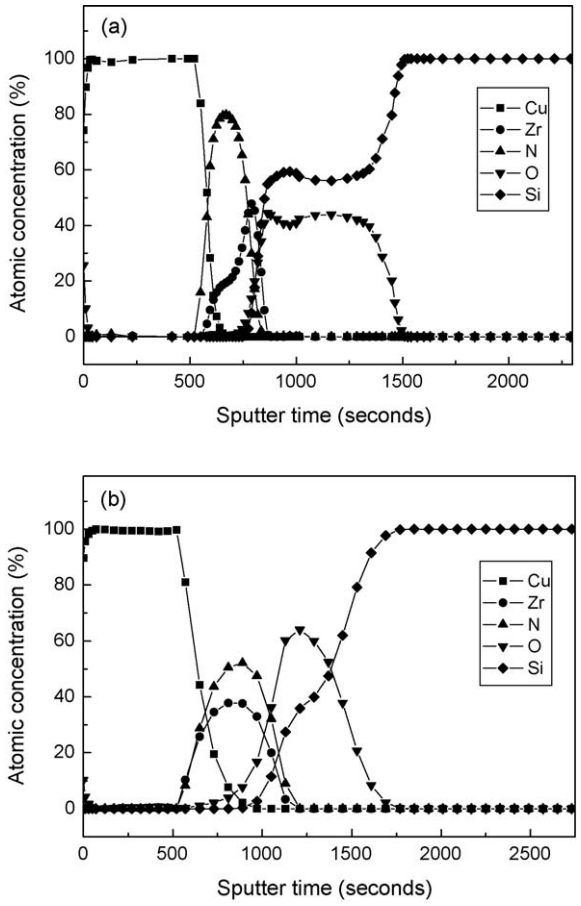

Fig. 9. AES depth profiles of Cu/ZrN(−200 V)/SiO_2/Si structures: (a) as-deposited and (b) annealed at 800 °C for 30 min.

bombardment effects. The failure temperature of the ZrN films with extremely thin thickness (above 800 °C), in the present study, was higher than that value above of 550 and 500 °C reported by Cho et al. [3] and Sato et al. [13], respectively.

4. Conclusion

Under energized ion bombardment, the resputtering phenomenon had significant influence on the deposition rate and impurity oxygen contents in the reactively sputtered ZrN films. The textures of ZrN films changed from (1 1 1) preferred orientation to (2 0 0) preferred orientation and then back to highly (1 1 1) preferred orientation, with increasing negative bias voltage, due to the competition between surface energy and strain energy. The evolution of electrical resistivity, as a function of substrate bias, depended on the impurity oxygen content in the films and the energy of ion bombardment irradiated on film surface. The reduction of impurity oxygen content and the densification of films, resulting from ion bombardment, could decrease the resistivity of ZrN films to 1.3 μΩ m. The results of sheet resistance and AES analysis revealed the feasibility of using ultra-thin ZrN films (10 nm), with negative bias of 200 V, as a diffusion barrier layer between Cu and SiO_2 up to 800 °C.

Acknowledgement

The authors would like to thank the National Science Council of the Taiwan, Republic of China, for its financial support under Contract No. NSC 96-2218-E006-006.

References

[1] T. Nitta, T. Ohmi, T. Hoshi, S. Sakai, K. Sakaibara, S. Imai, T. Shibata, Evaluating the large electromigration resistance of copper interconnects employing a newly developed accelerated life-test method, J. Electrochem. Soc. 140 (4) (1993) 1131–1137.
[2] S.K. Rha, W.J. Lee, S.Y. Lee, D.W. Kim, C.O. Park, S.S. Chun, Inter-diffusions and reactions in Cu/TiN/Ti/Si and Cu/TiN/Ti/SiO_2/Si multilayer structures, J. Mater. Res. 12 (12) (1997) 3367–3372.
[3] Seungchan Cho, Keunwoo Lee, Pungkeun Song, Hyeomgtag Jeon, Yangdo Kim, Barrier characteristics of ZrN films deposited by remote plasma-enhanced atomic layer deposition using tetrakis(diethylamino)-zirconium precursor, Jpn. J. Appl. Phys. 46 (7A) (2007) 4085–4088.
[4] Nam-Jin Bae, Kyoung-Il Na, Hyun-Ick Cho, Ki-Yeol Park, Sung-Eun Boo, Jeung-Ho Bae, Jung-Hee Lee, Thermal and electrical properties of 5-nm-thick TaN film prepared by atomic layer deposition using a pentakis(ethylmethylamino)tantalum precursor for copper metallization, Jpn. J. Appl. Phys. 45 (12) (2006) 9072–9074.
[5] Chin-An Chang, Chao-Kun Hu, Reaction between Cu and $TiSi_2$ across different barrier layers, Appl. Phys. Lett. 57 (6) (1990) 617–619.
[6] S.Q. Wang, Barriers against copper diffusion into silicon and drift through silicon dioxide, Mater. Res. Soc. Bull. 19 (8) (1994) 30–40.
[7] T.B. Massalski, Binary Phase Diagram, American Society for Metals, Westerville, OH, 1990.
[8] D.G. Gromov, A.I. Mochalov, A.G. Klimovitskiy, A.D. Sulimin, E.N. Redichev, Approaches to diffusion barrier creation and trench filling for copper interconnection formation, Appl. Phys. A 81 (7) (2005) 1337–1343.
[9] K. Yoshimoto, F. Kaiya, S. Shinkai, K. Sasaki, H. Yanagisawa, Preparation of single-oriented (1 1 1)VN film with low-resistivity and its application as diffusion barrier between Cu and Si, Jpn. J. Appl. Phys. 45 (1A) (2006) 215–220.
[10] M.B. Takeyama, T. Itoi, K. Satoh, M. Sakagami, A. Noya, Application of thin nanocrystalline VN film as a high-performance diffusion barrier between Cu and SiO_2, J. Vac. Sci. Technol. B 22 (5) (2004) 2542–2547.
[11] M.B. Takeyama, A. Noya, K. Sakanishi, Diffusion barrier properties of ZrN films in the Cu/Si contact systems, J. Vac. Sci. Technol. B 18 (3) (2000) 1333–1337.
[12] H.O. Pierson, Handbook of Refractory Carbides and Nitrides: Properties, Characteristics, Processing, and Applications, Noyes Publications, New Jersey, 1996.
[13] M. Sato, M.B. Takeyama, E. Aoyagi, A. Noya, Application of extremely thin ZrN film as diffusion barrier between Cu and SiOC, Jpn. J. Appl. Phys. 47 (1) (2008) 620–624.
[14] M.K. Lee, H.S. Kang, Characteristics of TiN film deposited on stellite using reactive magnetron sputter ion plating, J. Mater. Res. 12 (9) (1997) 2393–2400.
[15] Kevin S. Robinson, Peter M.A. Sherwood, X-ray photoelectron spectroscopic studies of the surface of sputter ion plated films, Surf. Interface Anal. 6 (6) (1984) 261–266.
[16] M. Ohring, The Materials Science of Thin Films, Academic Press, San Diego, 1992, p. 131.
[17] C.P. Liu, H.G. Yang, Systematic study of the evolution of texture and electrical properties of ZrN_x thin films by reactive DC magnetron sputtering, Thin Solid Films 444 (2003) 111–119.
[18] R. Lohmann, E. Osterschulze, K. Thoma, H. Gartner, Analysis of r.f.-sputtered TiB_2 hard coatings by means of X-ray diffractometry and Auger electron spectroscopy, Mater. Sci. Eng. A 139 (1991) 259–263.
[19] J. Pelleg, L.Z. Zevin, S. Lungo, Reactive-sputter-deposited TiN films on glass substrates, Thin Solid Films 197 (1991) 117–128.

[20] U.C. Oh, J.H. Je, Effects of strain energy on the preferred orientation of TiN thin films, J. Appl. Phys. 74 (3) (1993) 1692–1696.
[21] W. Ensinger, Growth of thin films with preferential crystallographic orientation by ion bombardment during deposition, Surf. Coat. Technol. 65 (1994) 90–105.
[22] M. Marinov, Thin Solid Films 46 (1977) 5267.
[23] B.S. Yau, J.L. Huang, M.C. Kan, Effects of substrate bias on nanocrystal-(Ti,Al)N_x/amorphous-SiN_y composite films, J. Mater. Res. 18 (8) (2003) 1985–1990.
[24] H.P. Klug, L.E. Alexander, X-Ray Diffraction Procedures, Wiley, New York, 1974.
[25] G. Hakansson, J.E. Sundgren, Microstructure and physical properties of polycrystalline metastable $Ti_{0.5}Al_{0.5}N$ alloys grown by D.C. magnetron sputter deposition, Thin Solid Films 153 (1987) 55–65.
[26] A. Cavaleiro, M.T. Vieira, G. Lemperiere, Influence of deposition conditions on the morphology of sputtered W–C–(Co) films, Thin Solid Films 213 (1992) 6–12.
[27] R.D. Bland, G.J. Kominiak, D.M. Mattox, Effect of ion bombardment during deposition on thick metal and ceramic deposits, J. Vac. Sci. Technol. 11 (4) (1974) 671–674.
[28] M. Ohring, The Materials Science of Thin Films, Academic Press, San Diego, 1992, p. 456.
[29] S.H. Wang, C.C. Chang, J.S. Chen, Effects of substrate bias and nitrogen flow ratio on the resistivity, density, stoichiometry, and crystal structure of reactively sputtered ZrN_x thin films, J. Vac. Sci. Technol. A 22 (5) (2004) 2145–2151.
[30] J.H. Huang, C.Y. Hsu, S.S. Chen, G.P. Yu, Effect of substrate bias on the structure and properties of ion-plated ZrN on Si and stainless steel substrates, Mater. Chem. Phys. 77 (2002) 14–21.
[31] K.C. Park, K.B. Kim, The effect of density and microstructure on the performance of TiN barrier films in Cu metallization, J. Appl. Phys. 80 (10) (1996) 5674–5681.
[32] W.H. Lee, Y.L. Kuo, H.J. Huang, C.P. Lee, Effect of density on the diffusion barrier property of TiN_x films between Cu and Si, Mater. Chem. Phys. 85 (2004) 444–449.
[33] J.W. Lim, K. Mimura, M. Isshiki, Suppression of Cu agglomeration in the Cu/Ta/Si structure by capping layer, Sci. Technol. Adv. Mater. 4 (2003) 391–396.
[34] C.C. Chang, J.S. Chen, W.S. Hsu, Failure mechanism of amorphous and crystalline Ta–N films in the Cu/Ta-N/Ta/SiO_2 structure, J. Electrochem. Soc. 151 (11) (2004) G746–G750.
[35] K.C. Park, S.H. Kim, K.B. Kim, Effect of ion bombardment during chemical vapor deposition of TiN films, J. Electrochem. Soc. 147 (7) (2000) 2711–2717.